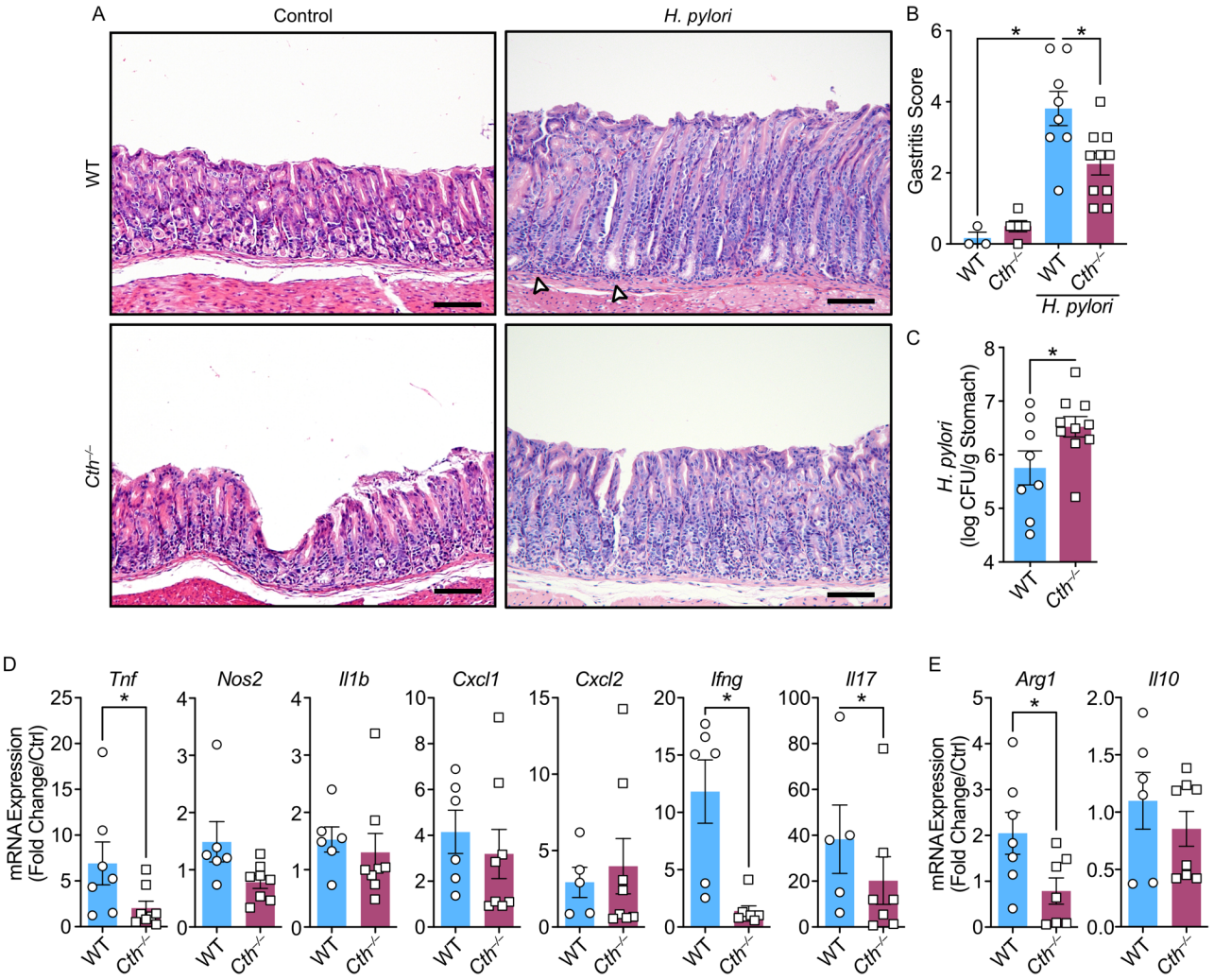

Supplemental Figure 1. *Cth*$^{-/-}$ mice exhibit decreased inflammation that is associated with decreased inflammatory gene expression. WT and *Cth*$^{-/-}$ mice were infected or not with *H. pylori* PMSS1 for 4 wk. (**A**) Representative H&E images of the gastric tissue. (**B**) Histologic gastritis scores, each symbol is a different mouse. (**C**) *H. pylori* colonization in gastric tissues from *B*. mRNA expression of (**D**) Pro-inflammatory, and (**E**) anti-inflammatory genes were assessed in the gastric tissues of WT and *Cth*$^{-/-}$ mice by RT-real-time PCR, n = 3-5 uninfected and 5-9 infected mice per genotype. All values are means ± SEM. Statistical analyses where shown: (**B**), (**D**), and (**E**) One-way ANOVA with Kruskal-Wallis test, followed by a Mann-Whitney U test; (**C**) Student's t test; *$p < 0.05$, **$p < 0.01$, and ***$p < 0.001$. Scale bars in (**A**), 50 µm.

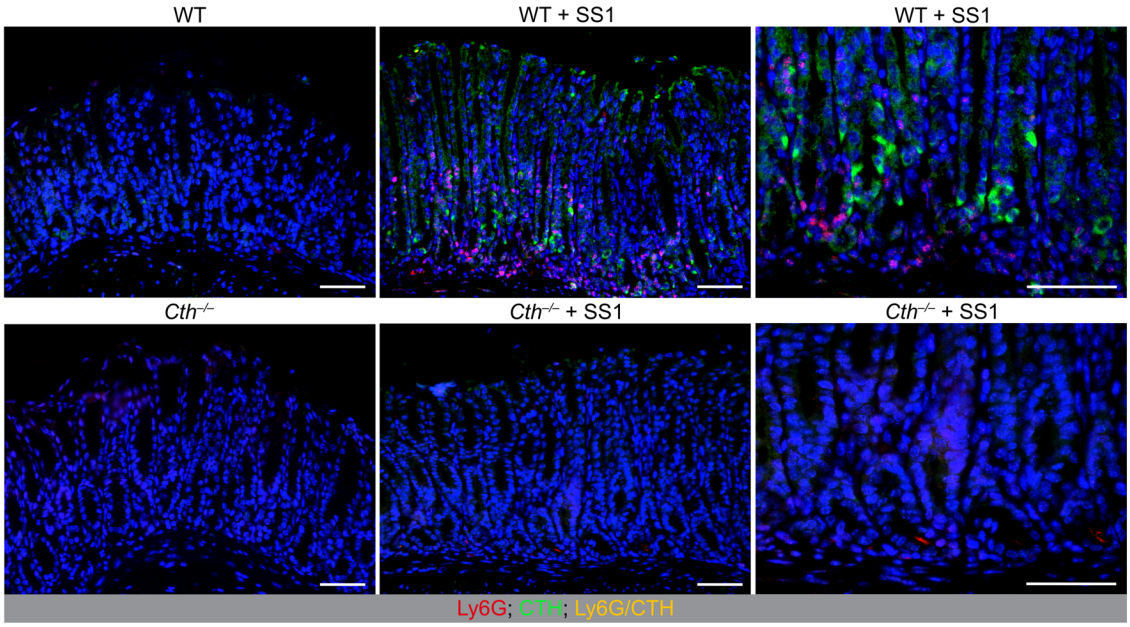

Supplementary Figure 2. Gastric neutrophils do not express CTH. Representative immunofluorescence images of gastric tissues from WT and *Cth*$^{-/-}$ mice infected or not with *H. pylori* SS1 for 16 wk; n = 3 mice per genotype. CTH (green); Ly6G (red); DAPI (blue). Scale bars; 50 μm.

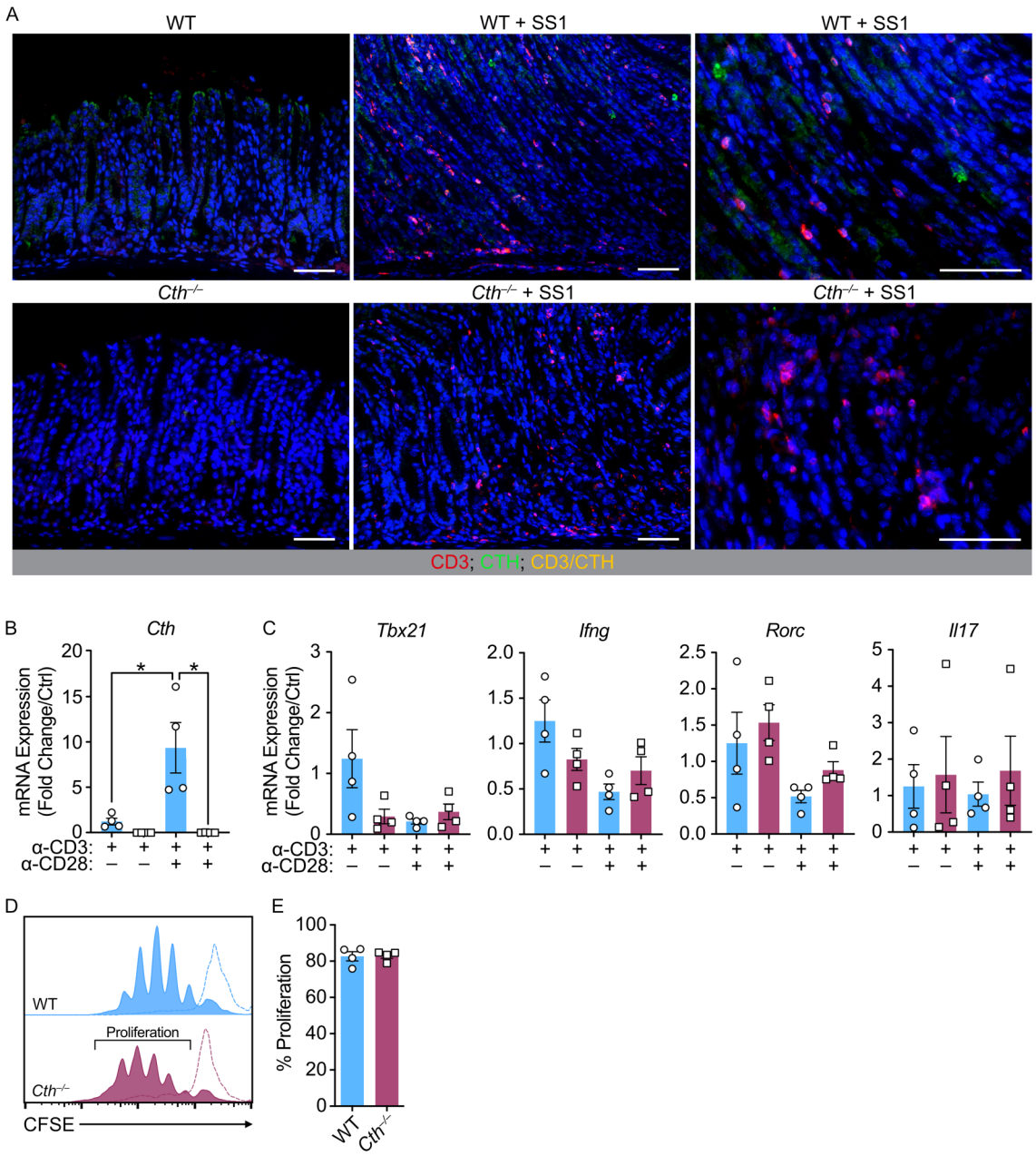

Supplementary Figure 3. Gastric T lymphocytes do not exhibit induced expression of CTH, and CD4$^+$ T cells do not rely on CTH for activation. (**A**) Representative immunofluorescence images of gastric tissues from WT and *Cth*$^{-/-}$ mice infected or not with *H. pylori* SS1 for 16 wk; $n = 3$ mice per genotype. CTH (green); CD3 (red); DAPI (blue). (**B-E**) Naïve CD4$^+$ splenocytes were isolated from WT and *Cth*$^{-/-}$. Cells were activated with α-CD3 or α-CD3+α-CD28 for 72 h; $n = 4$ mice per genotype. (**B**) mRNA expression of *Cth*. (**C**) mRNA expression of Th1 and Th17 transcription factors and cytokines. (**D**) Representative plot and (**E**) and quantification of proliferation as a percent of CFSE positive cells below baseline. Scale bars in (**A**), 50 μm.

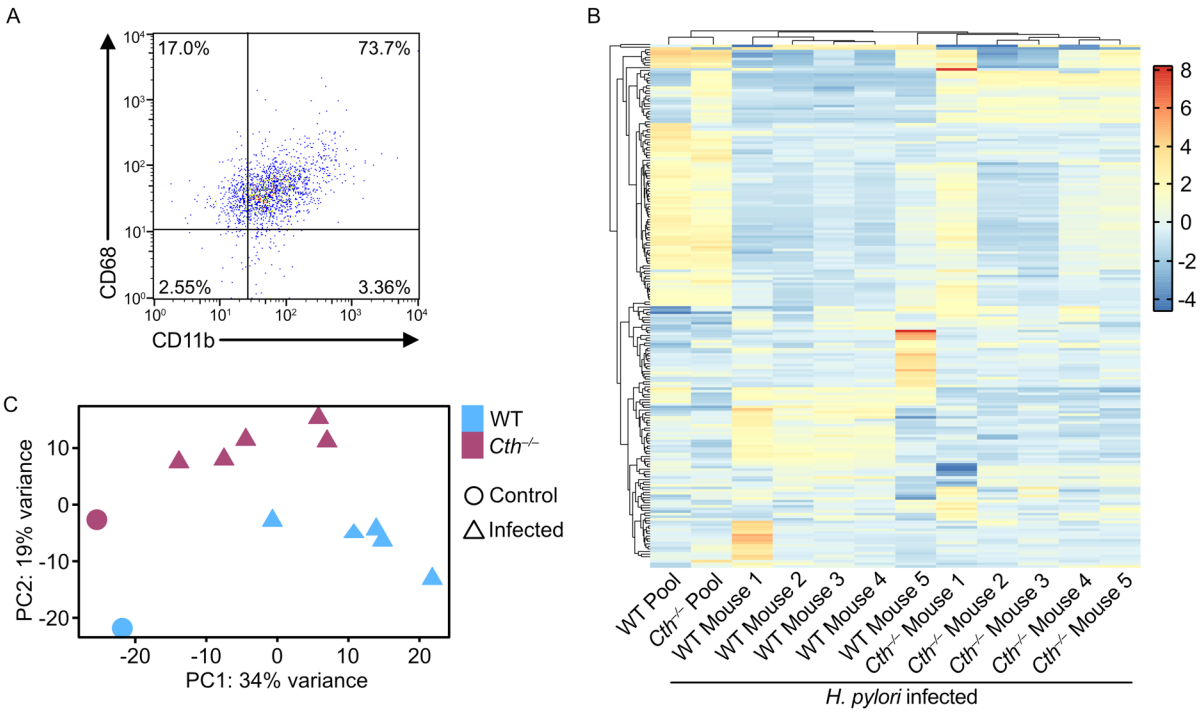

Supplemental Figure 4. RNA sequencing of F4/80^{+}-enriched gastric macrophages. (**A**) Representative plot of CD68 and CD11b expression from cells post-F4/80 positive selection from the gastric lamina propria**.** (**B**) Top 200 most variable genes at 16 wk p.i. with *H. pylori* SS1, *n* = pooled cells from uninfected mice and 5 individual infected mice per genotype. (**C**) PCA showing separate overall distribution between samples with different genotypes and infection status.

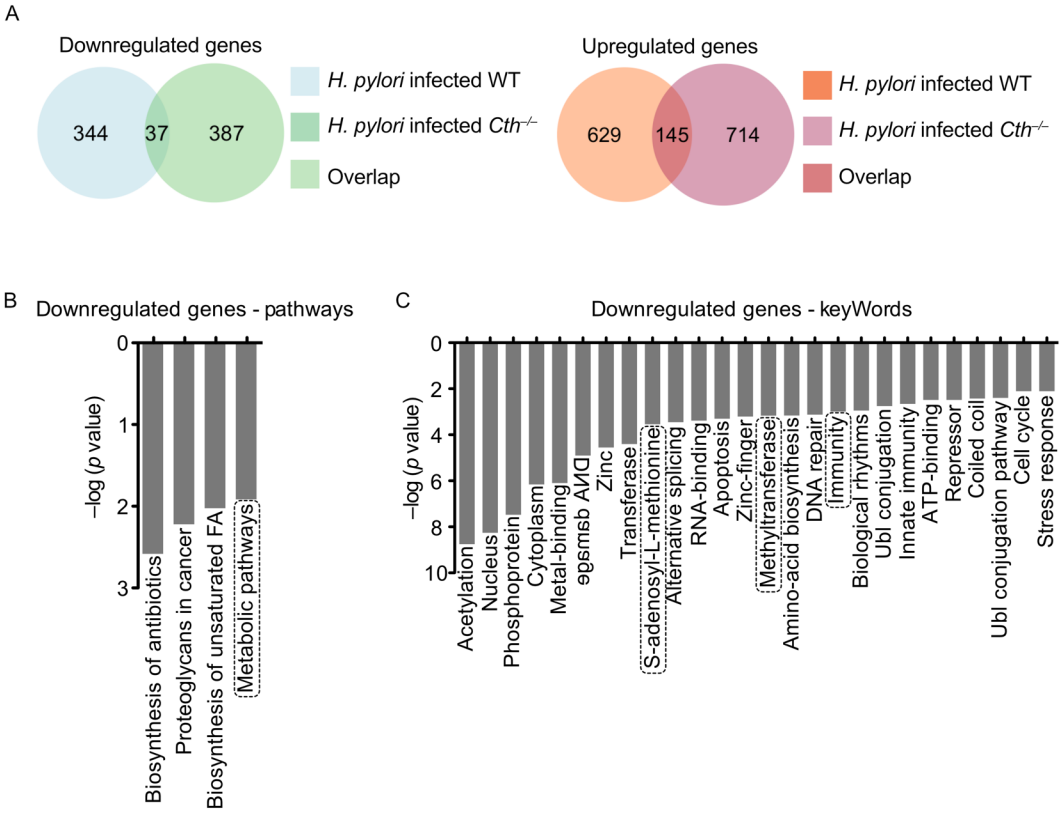

Supplemental Figure 5. Pathway analysis of DEGs downregulated by *H. pylori* infection using DAVID. (**A**) Venn diagrams showing abundance of commonly downregulated and upregulated genes in infected WT and *Cth*$^{-/-}$ mice compared to uninfected controls. (**B**) Significantly downregulated KEGG pathways. (**C**) Significantly downregulated KeyWords.

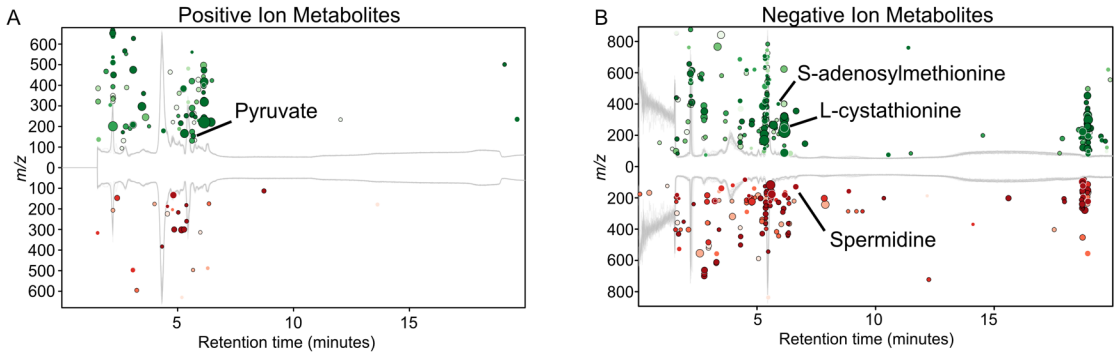

Supplemental Figure 6. Untargeted metabolomics and polyamine levels of WT and *Cth*$^{-/-}$ gastric tissues. Metabolomic analysis of gastric tissues from WT and *Cth*$^{-/-}$ mice at 8 wk p.i. with *H. pylori* PMSS1, $n = 8$ *H. pylori* PMSS1-infected mice per genotype. Cloud plots for the (**A**) positive ion and (**B**) negative ion metabolites downregulated (red) and upregulated (green) generated using XCMS. The x-axis represents the retention time, and the y-axis represents mass-to-charge ration (m/z). The fold change and *p* value are represented by dot size and shade, respectively.

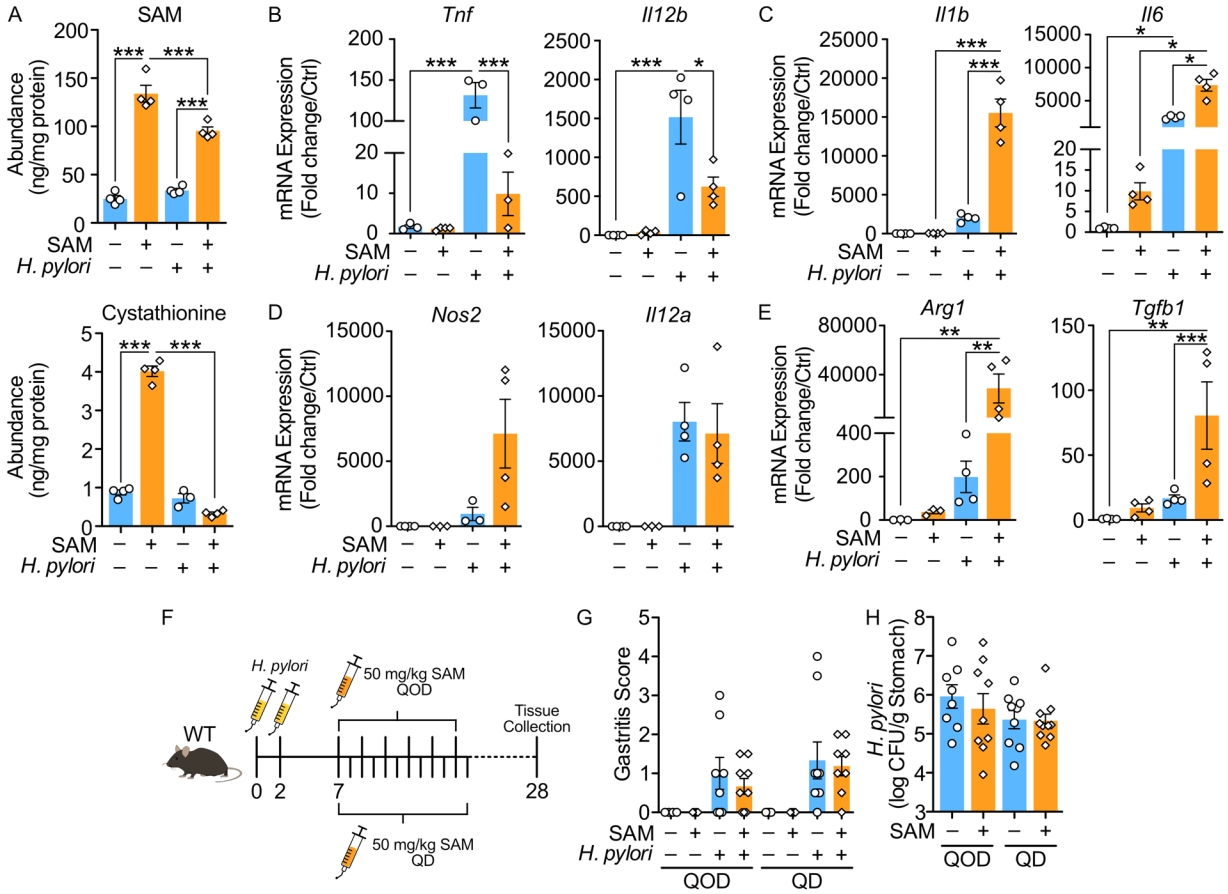

Supplemental Figure 7. SAM treatment does not confer protection against *H. pylori*-induced gastritis. (**A**) SAM and cystathionine levels in BMmacs 24 h p.i. with *H. pylori* ± 0.5 mM SAM; $n = 4$ biological replicates. Expression of pro-inflammatory genes (**B**) decreased, (**C**) increased, and (**D**) unchanged by SAM treatment 24 h p.i. with *H. pylori*, $n = 4$ biological replicates. (**E**) Expression of anti-inflammatory genes increased with by SAM treatment treatment 24 h p.i. with *H. pylori*, $n = 4$ biological replicates. (**F**) C57BL/6 mice infected or not with *H. pylori* PMSS1 ± 50 mg/kg SAM every other day (QOD) or every day (QD) for 4 wk; $n = 9$-10 infected mice per treatment. (**G**) Histologic gastritis scores. (**H**) *H. pylori* colonization in gastric tissues from *G*. All values are means ± SEM. Statistical analyses where shown: (**A-C**) and (**E**) One-way ANOVA with Kruskal-Wallis test, followed by a Mann-Whitney *U* test; *$p < 0.05$, **$p < 0.01$, and ***$p < 0.001$.

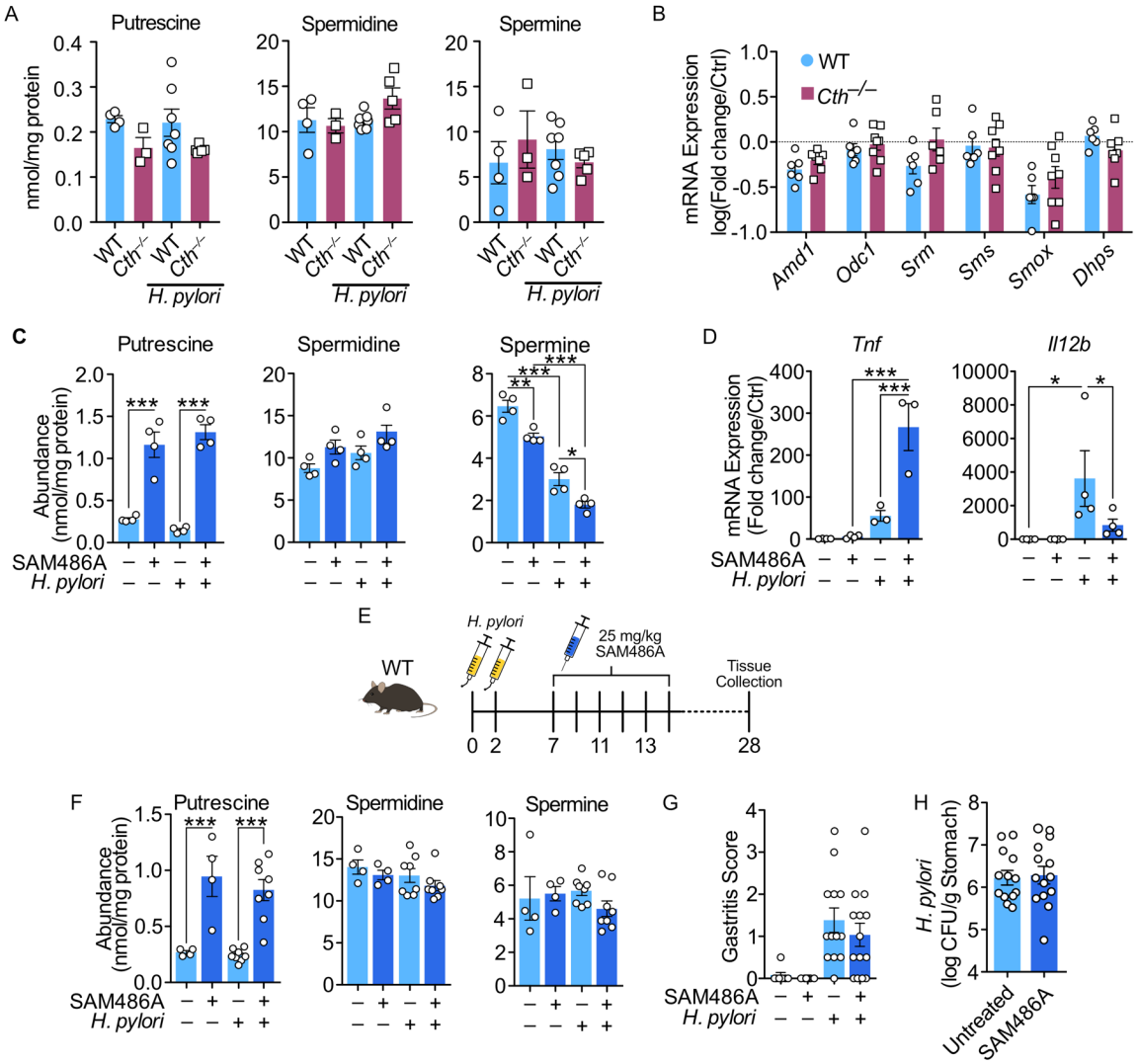

Supplemental Figure 8. SAM486A treatment does not confer protection against *H. pylori*-induced gastritis. (**A**) Polyamine levels were measured by LC-MS in the gastric tissues of WT and *Cth*$^{-/-}$ mice at 16 wk p.i. with *H. pylori* SS1, n = 3-4 uninfected and 5-6 *H. pylori* SS1-infected mice per genotype. (**B**) mRNA expression of enzymes involved in polyamine biosynthesis and metabolism in the gastric tissues of WT and *Cth*$^{-/-}$ mice at 4 wk p.i. with *H. pylori* PMSS1, n = 3-5 uninfected and 6-8 infected mice per genotype. (**C**) Polyamine levels in BMmacs 24 h p.i. with *H. pylori* ± 1 μM SAM486A; n = 4 biological replicates. (**D**) Gene expression of pro-inflammatory genes upregulated by SAM486A treatment 24 h p.i. with *H. pylori*; n = 4 biological replicates. (**E**) C57BL/6 mice infected or not with *H. pylori* PMSS1 ± 5 mg/kg SAM486A for 4 wk; n = 4-6 uninfected and 8-10 infected mice per treatment from 2 independent experiments. (**F**) Polyamine levels in gastric tissues; n = 4 uninfected and 8 infected mice per treatment. (**G**) Histologic gastritis scores. (**H**) *H. pylori* colonization of in gastric tissues in *G* All values are means ± SEM. Statistical analyses where shown: (**C**) and (**F**), One-way ANOVA with Newman-Keuls post hoc test; (**D**), One-way ANOVA with Kruskal-Wallis test, followed by a Mann-Whitney *U* test; *$p < 0.05$, **$p < 0.01$, and ***$p < 0.001$.

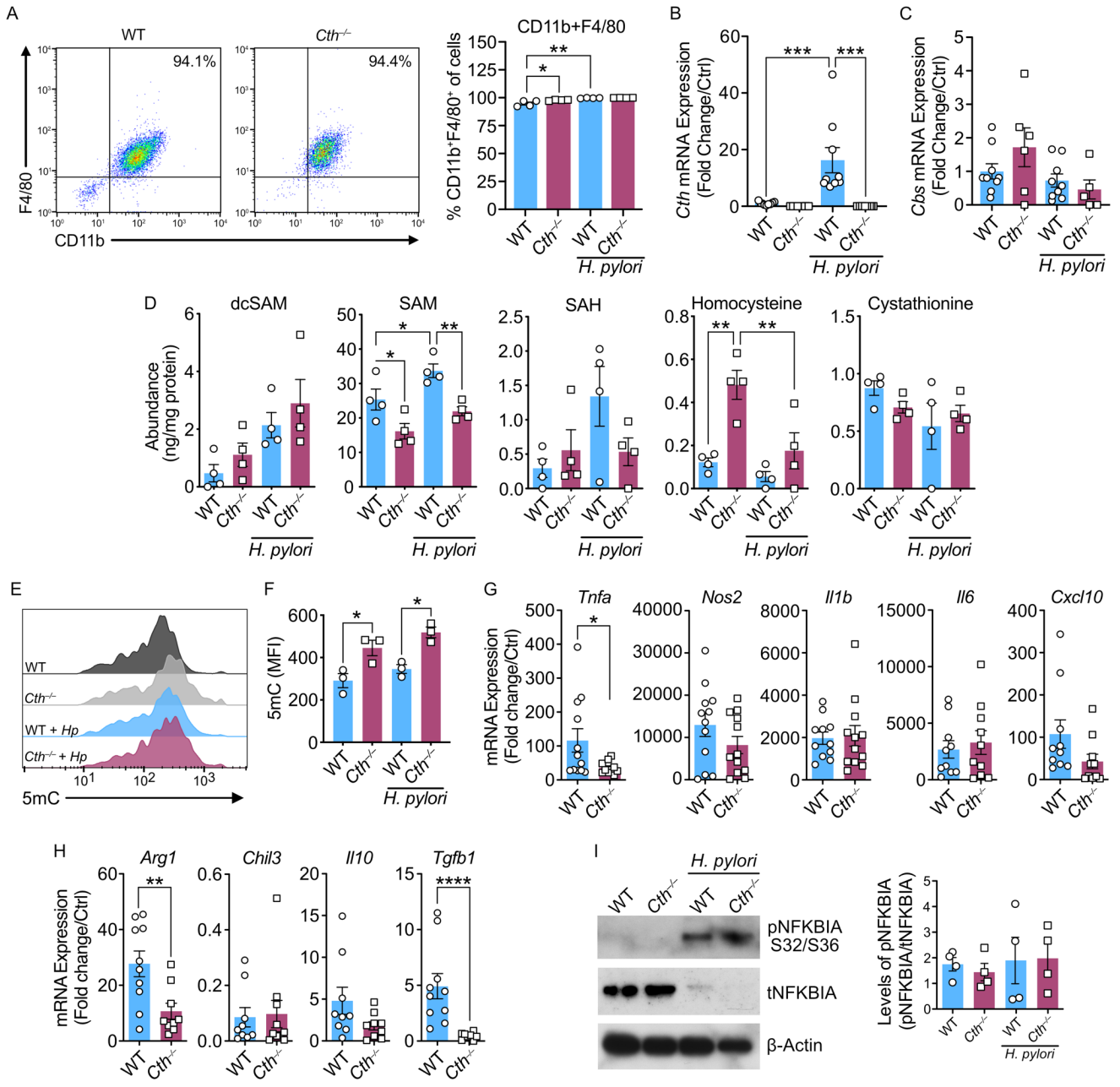

Supplemental Figure 9. (**A**) Representative plot of uninfected cells and quantification of the precent of $CD11b^{+}F4/80^{+}$ cells shown in Figure 6B, $n = 4$ biological replicate per genotype. (**B**) Expression of *Cth* by WT and $Cth^{-/-}$ BMmacs 24 h p.i. with *H. pylori*, $n = 9$ biological replicates from 3 independent experiments (WT are the same as in Figure 6A). (**C**) Expression of *Cbs* by WT and $Cth^{-/-}$ BMmacs 24 h p.i. with *H. pylori*, $n = 6$-9 biological replicates from 3 independent experiments. (**D**) Abundance of metabolites shown in Figure 6C. $n = 4$ biological replicates. (**E**) Representative plot of WT and $Cth^{-/-}$ BMmacs stained with 5mC 24 h p.i. with *H. pylori*. (**F**) Quantification of the MFI in *E*. $n = 3$ biological replicates per genotype. mRNA expression of pro-inflammatory (**G**) and anti-inflammatory (**H**) genes by WT and $Cth^{-/-}$ BMmacs 24 h p.i. with *H. pylori*, $n = 4$-10 biological replicates per genotype from 3 independent experiments. (**I**) pNFKBIA immunoblots and densitometric analysis of WT and $Cth^{-/-}$ BMmacs 30 min p.i. with *H. pylori*, $n = 3$-4 biological replicates from 2 independent experiments. All values are means ± SEM. Statistical analyses where shown: One-way ANOVA with Newman-Keuls test, followed by a Mann-Whitney *U* test; $*p < 0.05$, $**p < 0.01$, $***p < 0.001$.

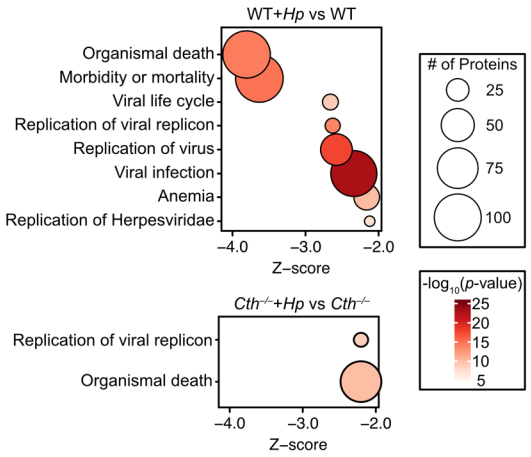

Supplemental Figure 10. Proteomic pathways downregulated by *H. pylori* infection in BMmacs. Enrichment analysis of pathways inhibited by *H. pylori* infection in WT and *Cth*$^{-/-}$ BMmacs., n = 4 biological replicates per genotype. (FDR <0.05, z-score <-2).

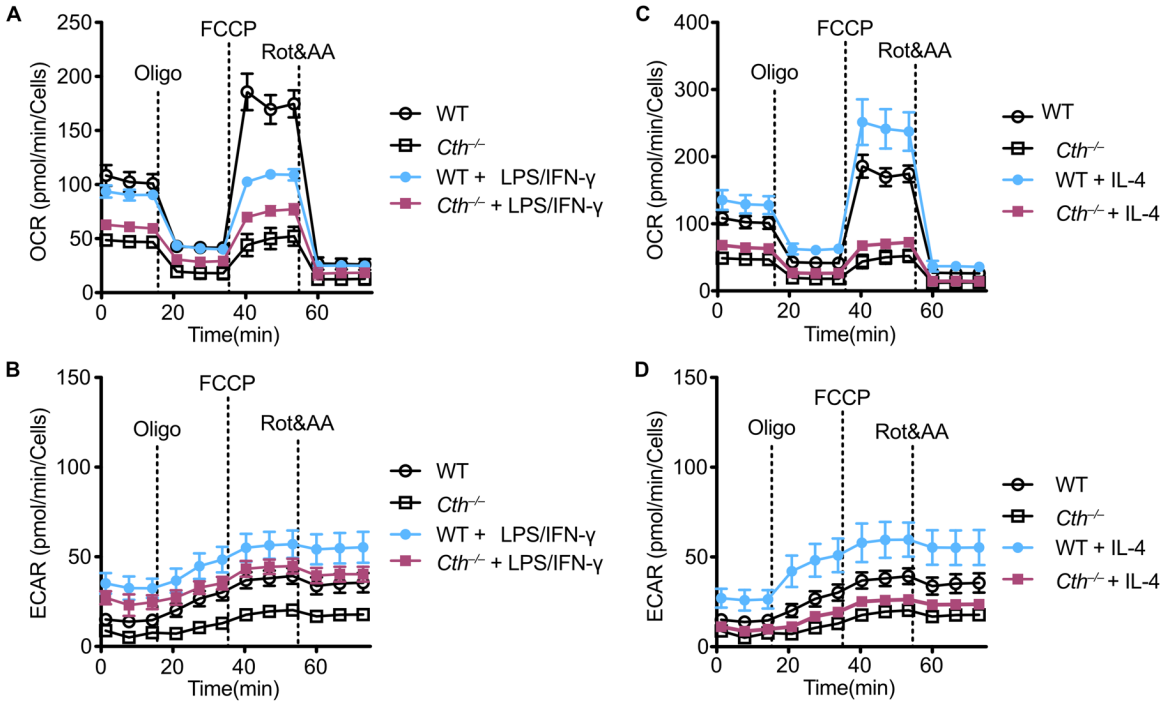

Supplemental Figure 11. Cellular respiration of classically stimulated WT and *Cth*$^{-/-}$ BMmacs. (**A-B**) WT and *Cth*$^{-/-}$ BMmacs stimulated with LPS (10 ng/mL) and IFNγ (200 U/mL). (**A**) Oxygen consumption rate and (**B**) extracellular acidification rate assessed 24 h post-stimulation, $n = 5$ from 2 independent experiments. (**C-D**) WT and *Cth*$^{-/-}$ BMmacs stimulated with IL-4 (10 ng/mL). (**C**) Oxygen consumption rate and (**D**) extracellular acidification rate assessed 24 h post-stimulation, $n = 5$ from 2 independent experiments. Vertical dashed lines indicated the sequential addition of oligomycin (Oligo), FCCP, and Rot/AA (The controls are the same as in Figure 9). All values are means ± SEM.

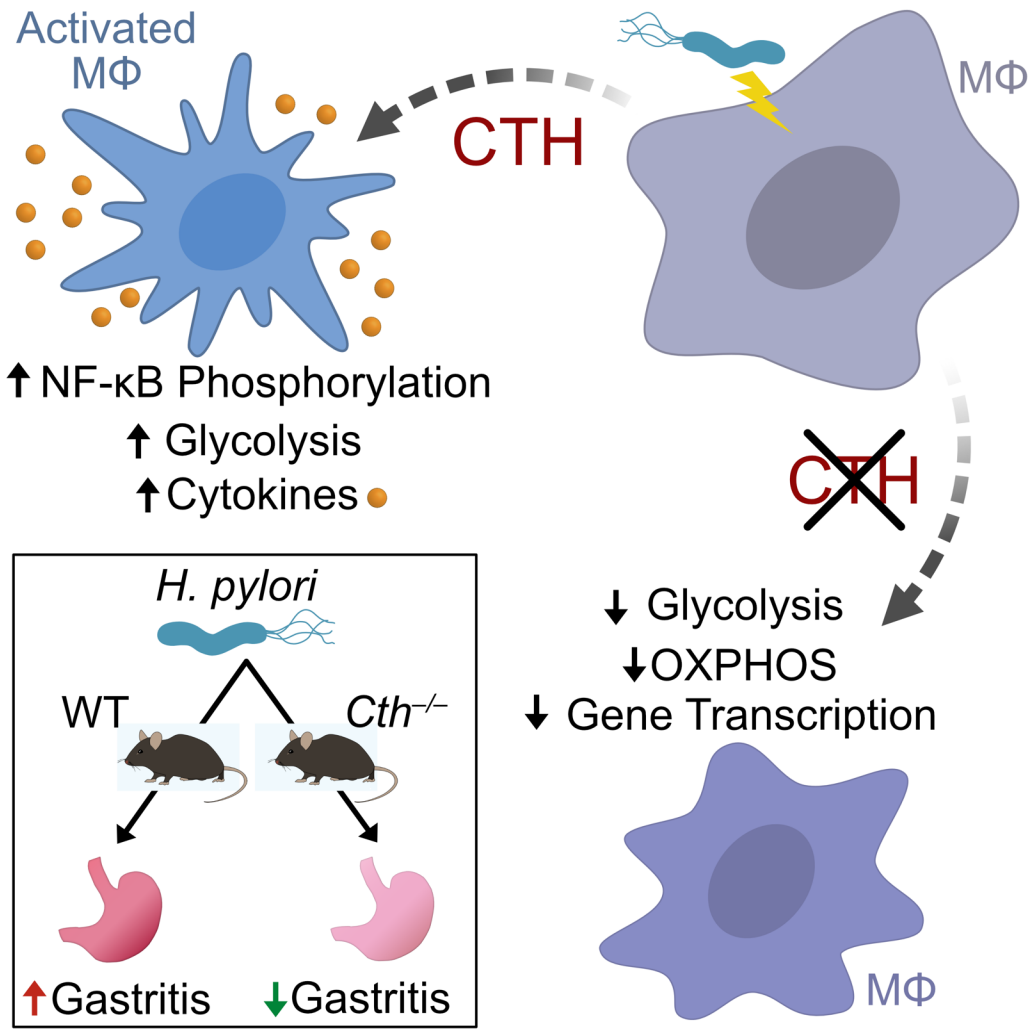

Supplemental Figure 12. Graphical summary of the role of CTH in the macrophage response to *H. pylori*. Macrophages upregulate the expression of *Cth* when infected with *H. pylori* leading to an increase in glycolysis and M1 activation which is attenuated in the absence of CTH. The abrogated macrophage activation in *Cth*$^{-/-}$ mice provides protection from *H. pylori*-induced gastric inflammation.

SUPPLEMENTAL DATASETS

Dataset 1. Full list of differentially expressed gene, including Ensemble transcript IDs, official gene symbols, fold-changes, and *p*-values for all four groups. (*n* = pooled cells from 10 uninfected mice and 5 individual *H. pylori* SS1 infected mice per genotype).

Dataset 2. Full lists of gene sets identified by GSEA performed on the DEG dataset between infected *Cth*$^{-/-}$ Gmacs and infected WT Gmacs presented in Dataset 1.

Dataset 3. Full lists of pathways identified by DAVID performed on the Interaction DEG dataset presented in Dataset 1.

Dataset 4. Full list of the pathways identified by the metabolomic analysis.

Dataset 5. Complete dataset of the proteomic analysis of BMmacs from WT (*n* = 3) and *Cth*$^{-/-}$ (*n* = 3) mice infected or not with *H. pylori*.

Dataset 6. Full lists of pathways identified by IPA performed on the WT proteome dataset presented in Dataset 5.

Dataset 7. Full lists of pathways identified by IPA performed on the *Cth*$^{-/-}$ proteome dataset presented in Dataset 5.

SUPPLEMENTAL METHODS

Animal Studies. *Cth*$^{-/-}$ mice were generated and provided by Bindu Paul and Solomon Snyder, Johns Hopkins University School of Medicine (Baltimore, MD) (1). C57BL/6 wild-type (WT, also provided by BDP and SHS) and *Cth*$^{-/-}$ mice were house-bred and maintained for multiple generations in the same room of our animal facility prior to experiments. Adult age-matched WT and *Cth*$^{-/-}$ mice (8-12 wk) of both sexes were used for isolation of BMmacs and for infection with *H. pylori*. Mice remained in the cages they were weaned in and moved to the same rack for infection studies.

Bone Marrow-Derived Macrophage Culture. Bone marrow cells were isolated from mice of both genotypes as previously described (2) with the following exception; prior to counting, RBCs were lysed with ACK Lysing Buffer (ThermoFisher) for 1 minute. Cells were differentiated into BMmacs for 7 days in complete medium (DMEM media supplemented with 10% FBS, 100 U/ml penicillin/streptomycin, 25 mM HEPES, and 20 ng/ml recombinant macrophage CSF (M-CSF; PeproTech)).

CD4$^+$ Splenocyte Culture and Proliferation Analysis. Naïve CD4+ cells were isolated from the spleens of WT and *Cth*$^{-/-}$ mice using the Dynabeads Untouched Mouse CD4 Cells Kit (Thermo Fisher). Cells were seeded into plates pre-coated with 5 μg/mL α-CD3e (Thermo Fisher) and stimulated or not with 2.5 μg/mL of soluble α-CD28 (Thermo Fisher). Cells were maintained for 72 h in complete media (RMPI media supplemented with 10% FBS, 100 U/ml penicillin/streptomycin, 25 mM HEPES, and 50 μM β-mercaptoethanol (βME)).

Proliferation was assessed using CFSE staining and flow cytometry. Briefly, immediately after CD4$^+$ splenocyte isolation, cells were incubated with 25 μM CFSE for 5 min at room temperature. Cells were then washed and plated as above. After 72 h, cells were collected and subsequently analyzed by flow cytometry.

Bacteria. The *cagA+ H. pylori* strain PMSS1 and the mouse-adapted *H. pylori* strain SS1 were grown on Trypticase soy agar (TSA) plates containing 10% sheep blood (3–5). Bacteria were harvested directly from plates to infect the macrophages. For *in vivo* infection, *H. pylori* was grown from plates in Brucella broth containing 10% FBS overnight; *H. pylori* was then diluted, grown, and harvested at the exponential phase. *C. rodentium* (2) was grown in Luria-Bertani broth overnight to infect macrophages.

Infection. Mice were infected twice by oral gavage, on day 0 and day 2, with 10^9 *H. pylori* PMSS1 or SS1 in 0.2 mL Brucella broth (5). Control mice were treated with 0.2 mL Brucella broth alone. Mice were fed *ad libitum* with regular 5L0D chow (LabDiet). Animals were sacrificed after 4 and 8 wk (PMSS1) or 16 wk (SS1). Stomachs

were harvested and analyzed as previously described (2, 4, 6, 7). *H. pylori* gastric colonization was determined by counting the CFUs after plating serial dilutions of homogenized tissues.

Animals were treated or not with 50 mg/kg SAM (S-(5′-adenosyl)-L-methionine chloride dihydrochloride, Sigma-Aldrich) by oral gavage (8) during 4 wk PMSS1 experiments beginning 1 wk p.i.. Animals were treated either every other day or every day. Solutions were prepared immediately prior to each treatment. Animals were treated or not with 5 mg/kg SAM486A (Sardomozide, MedChemExpress) by IP injection (9) every other day during 4 wk PMSS1 experiments beginning 1 wk p.i.. Control mice were treated with vehicle.

Quantitative Real-Time PCR (RT-PCR). Total RNA was isolated from macrophages using the RNeasy Mini Kit (QIAGEN). RNA was extracted from mouse tissues by homogenization in TRIzol. cDNA was synthesized using the SuperScript IV Reverse Transcriptase (Thermo Fisher) and Oligo dT (Thermo Fisher). mRNAs were amplified by real-time PCR using the PowerUp SYBR Master Mix (Thermo Fisher) and the primers listed in Supplemental Methods, Table S4.

Immunostaining. Immunofluorescent staining for CTH and the macrophage marker CD68 was performed on murine gastric tissues as described (10) using the following antibodies (see Supplemental Methods, Table S3): Rabbit polyclonal anti-CTH, 1/100; rabbit polyclonal anti-mouse CD68, 1/100, ready to use; rabbit monoclonal anti-mouse Ly6G, 1/100; rabbit monoclonal anti-mouse CD3, 1/100, ready to use; goat anti-rabbit IgG, Alexa Fluor 488-labeled, 1/400; goat anti-rabbit IgG, Alexa Fluor 555-labeled, 1/500.

Histopathology. Histologic scoring was determined using the modified Sydney System (11) by a gastrointestinal pathologist (MBP) in a blinded manner. Gastritis was assessed on a longitudinal strip of tissue fixed in 10% neutral buffered formalin and stained with H&E. Acute and chronic inflammation were each scored 0–3 in the antrum and corpus regions, and the scores for antrum and corpus were added together for a 0–12 scale (7).

Gastric Macrophage Isolation and Enrichment Analysis. Macrophages were isolated from the gastric lamina propria as previously described (4, 12, 13). Briefly, at 16 wk p.i., the glandular portion of the stomach was removed, washed, cut into 2 mm pieces, and digested for 20 min with 1 mg/ml dispase and 0.25 mg/ml of collagenase A at 37°C while shaking. The cells were passed through a 70 μm cell strainer and harvested by centrifugation. Isolated cells were labeled with biotin-conjugated anti-mouse F4/80 antibody, 1/50, at 4°C for 1 h followed by incubation with streptavidin-conjugated beads at 4°C for 1 h. The cells were resuspended in 1 ml of buffer and underwent multiple rounds of washing while applied to a magnet. The positive selection was then collected and immediately used for RNA extraction. Since there are only a small number of gastric macrophages

present in uninfected mice, we pooled the F4/80-positive cells from ten mice for each control sample (13). Macrophage enrichment was assessed by pooling the F4/80-positive cells from three naïve WT mice. Cells were fixed and permeabilized with CytoFix/CytoPerm (BD Biosciences) for 20 mins at 4°C, washed, and then labeled with anti-CD11b-FITC (BD Biosciences), 1/200, and anti-CD68-PE, 1/200, (BioLegend), for 20 min at 4°C in Perm/Wash Buffer. Cells were then washed 3 times and subsequently analyzed using flow cytometry. See Supplemental Methods, Table S3 for information regarding antibodies used in this study.

RNA sequencing and Analysis. Total RNA was isolated from the F4/80^{+} gastric macrophages using the RNeasy Micro kit (QIAGEN). Generation and amplification of cDNA was performed using the Ovation RNA-Seq System V2 (Tecan). RNAseq library preparation and Next Generation Sequencing (PE150) were performed using the NEBNext Ultra II Directional RNA Library Prep Kit for Illumina (BioLabs, Inc.) and Illumina NovaSeq6000 with NovaSeq 6000 SP Reagent Kit (Illumina), respectively. Reads were first trimmed to remove the adapter sequence and read quality was checked using *fastp* (14). Transcripts were quantified and mapped to the indexed mouse genome (M23, GRCm38) using *Salmon* (15). Transcript-level quantification was then summarized to the gene level, annotated, and prepared for differential gene expression analysis using the R package *tximeta* (16). The R/Bioconductor package *DESeq2* was then used to identify differentially expressed genes in each condition using Benjamini-Hochberg (BH) adjustment (FDR $p < 0.05$) (17). DAVID was used for pathway analysis and functional annotation of DEGs (18, 19). GSEA was performed using the R packages *clusterProfiler* (20) and *DOSE* (21).
The RNA sequencing data that is included in this study have been deposited in NCBI Gene Expression Omnibus (accession number GEO: GSE158817).

***Untargeted Metabolomics*.** At 8 wk p.i., gastric tissues were processed, and untargeted metabolomics was performed as previously described (7). Gastric tissues were homogenized by sonication in water:methanol (9:1) containing 50 mM ammonium acetate (pH~6) to yield a tissue density of 50 mg/ml. An aliquot of the homogenate was combined with HPLC-grade methanol, vortexed vigorously, and centrifuged. A portion of the supernatant was diluted with an equal volume of HPLC-grade acetonitrile. A Vanquish ultrahigh performance liquid chromatography (UHPLC) system interfaced to a Q Exactive HF quadrupole/orbitrap mass spectrometer (Thermo Fisher Scientific) was used to acquire discovery metabolomics data. Each sample was first injected in positive ESI mode followed by a second injection in negative mode. All chromatographic separations were performed using a Zic-cHILIC analytical column (3 mm, 2.1 3 150 mm; Merck SeQuant). Mobile phases were made up of 0.2% acetic acid and 15 mM ammonium acetate in (A) water:acetonitrile (9:1) and in (B) acetonitrile:methanol:water (90:5:5). The total chromatographic run time was 20 min, the sample injection

volume was 10 ml, and the flow rate was maintained at 300 ml/min. Mass spectra were acquired over a precursor ion scan range of m/z 100 to 1,200 at a resolving power of 30,000 using the following ESI source parameters: spray voltage 5 kV (3 kV in negative mode); capillary temperature 300°C; S-lens RF level 60 V; N_2 sheath gas 40; N_2 auxiliary gas 10; auxiliary gas temperature 100°C. MS/MS spectra were acquired for the five most abundant precursor ions with an MS/MS AGC target of 105, a normalized collision energy of 30, and a maximum MS/MS injection time of 100 ms. Chromatographic alignment, peak picking, and statistical comparisons were performed using XCMS (https://xcmsonline.scripps.edu) (22).
The discovery metabolomics data has been deposited to EMBL-EBI MetaboLights (23) (accession number MetaboLights: MTBLS2851).

Targeted Metabolite Quantification. SAM, dcSAM, SAH, homocysteine, cystathionine, and cysteine were measured at the Vanderbilt Neurochemistry Core as previously described (10) and polyamine concentrations were measured as previously described (2). Briefly, cell pellets or flash frozen tissues were homogenized, and the supernatants were used for the BCA Protein Assay (Pierce) and for liquid chromatography-mass spectrometry (LC-MS). Isotopically-labeled internal standard solutions were used for sample analysis. LC was performed on a 2.0 x 100-mm, 1.7-µm-particle-size CORTECS UPLC Phenyl column (Waters Corporation, Milford, MA USA) using a Waters Acquity I-Class ultraperformance liquid chromatography (UPLC) system. Mobile phase A was 1% aqueous formic acid, and mobile phase B was acetonitrile. Samples were separated by a gradient of 98 to 5% mobile phase A over 11 min at a flow rate of 600 µl/min prior to delivery to a Waters Xevo TQ-S micro triple quadrupole mass spectrometer. The peak height of the endogenous metabolites was compared to the peak height of internal standards for quantitation.
All data were analyzed using TargetLynx XS software version 4.1 (Waters Corporation).

Co-Cultures. SAM and SAM486A were added to cells 30 minutes prior to infection. Macrophages were infected with *H. pylori* at a MOI of 100 for 30 min, 6 h, or 24 h. For *C. rodentium*, macrophages were infected at a MOI of 10 for 3 h and then washed and media containing penicillin and streptomycin was added for 21 h more. Media without antibiotics was used for all experiments. LPS/IFN-γ stimulated BMmacs were generated by addition of 10 ng/ml LPS from *E. coli* O111:E4 (Sigma-Aldrich) and 200 U/ml mouse recombinant IFN-γ (PeproTech). IL-4- and IL-10-stimulated BMmacs were generated with 10 ng/ml murine recombinant IL-4 (PeproTech) and 10 ng/ml murine recombinant IL-10 (PeproTech), respectively.

5mC Immunostaining and Flow Cytometry. 5mC immunostaining was performed as previously described (24) with the following exceptions; 24 h p.i., macrophages were washed with PBS and fixed and permeabilized using

the CytoFix/CytoPerm kit (BD Bioscience). Chromatin was denatured with 1N HCl for 1 h at 37°C. Non-specific antibody binding was minimized by blocking with Wash Buffer (BD Bioscience) supplemented with 10% FBS for 20 min at 37°C. Cells were then labeled with mouse monoclonal anti-5mC (Bio-Rad), 1/100, for 30 min at room temperature followed by washing and detection with goat anti-mouse IgG, Alexa Fluor 488-labeled, 1/200, for 45 min at 37°C. Upon completion of staining, 5mC binding was analyzed by flow cytometry; at least 10,000 cells were counted for each sample.

Proteomics and IPA. Macrophages were infected or not with *H. pylori* PMSS1 for 24 h and lysed in 50 mM Tris-HCl pH 7.6, 150 mM NaCl, 1% NP-40, and 2 mM EDTA and protein concentrations were determined by the BCA Protein Assay (Pierce). Samples within each group were combined (15 mg per each lysate), diluted with 100 mM triethylammonium bicarbonate (TEAB), reduced with 5 mL of 200 mM tris(2-carboxyethyl)phosphine (TCEP) at 55°C for 1 h, and carbamidomethylated with 5 mL of 375 mM iodoacetamide for 30 m in the dark at room temperature. Proteins were precipitated with cold acetone, and precipitates were dried and reconstituted in 100 mM TEAB (pH 8.0). Proteins were digested with Trypsin Gold (Promega) overnight at 37°C. Quantitative proteomics analysis was performed using TMT Isobaric Mass Tagging reagents (Thermo Fisher) according to the manufacturer's instructions. Peptides were labeled with TMT reagents with each reconstituted protein sample being labeled with an individual vial of 0.8 mg TMTsixplex reagent (Thermo Fisher). After labeling was complete, labeled peptides from each of the 4 sample groups were combined and fractionation was performed with 40 mg of the combined mixture using the Pierce High pH Reversed-Phase Peptide Fractionation Kit (Thermo Fisher) similar to the manufacturer's recommended protocol for TMT-labeled peptides. Elution steps consisted of the following: 10%, 12.5%, 15%, 17.5%, 20%, 22.5%, 25%, 50%, and 80% acetonitrile with 0.1% triethylamine. Eluted fractions were dried via vacuum centrifugation in a SpeedVac concentrator, and peptides were reconstituted in 0.1% formic acid for analysis by LC-coupled tandem mass spectrometry (LC-MS/MS). An analytical column was packed with 30 cm of C18 reverse phase material (Jupiter, 3 µm beads, 300 Å, Phenomenox) directly into a laser-pulled emitter tip. Peptides were loaded on the capillary reverse phase analytical column (360 µm O.D. x 100 µm I.D.) using a Dionex Ultimate 3000 nanoLC and autosampler. The mobile phase solvents consisted of 0.1% formic acid, 99.9% water (solvent A) and 0.1% formic acid, 99.9% acetonitrile (solvent B). Peptides were gradient-eluted at a flow rate of 400 nL/min, using a 155-min gradient. The gradient consisted of the following: 5-30% B in 125 min, 30-50% B in 10 min, 50-70% B in 4 min, 70% B for 2 min; 70-2% B in 2 min, followed by column equilibration. A Q Exactive Plus mass spectrometer (Thermo Scientific), equipped with a nanoelectrospray ionization source, was used to mass analyze the eluting peptides using a data-dependent method. The instrument method consisted of MS1 using an MS AGC target value of

$3x10^6$, followed by up to 15 MS/MS scans of the most abundant ions detected in the preceding MS scan with an MS2 AGC target of $1x10^5$. Dynamic exclusion was set to 20 s, HCD collision energy was set to 30 nce, and peptide match and isotope exclusion were enabled. For the final two fractions, the peptides were eluted from the reverse phase analytical column using a gradient of 5-50% B in 125 min, followed by 50-95% B in 12 min, 95% B for 1 min, 95-5% B in 2 min, and column equilibration at 2% B.

For identification of peptides, HCD tandem mass spectra were searched in Proteome Discoverer 2.1 (Thermo Scientific) using SequestHT for database searching against a subset of the UniprotKB protein database (www.uniprot.org) containing *Mus musculus* protein sequences. The factory default templates in Proteome Discoverer were used for processing and consensus workflows, which included the PWF_QE_Reporter_Based_Quan_SequestHT_Percolator processing workflow and the CWF_Comprehensive_Enhanced Annotation_Quan_Results export consensus workflow. Search parameters included trypsin cleavage rules with two missed cleavage sites, carbamidomethyl (C) and TMTsixplex (K, N-terminus) as static modifications, and a dynamic modification of oxidation (M). Percolator validation was performed with a target false discovery rate (FDR) setting of 0.01 for high confidence protein identifications. A few exceptions to the consensus workflow default settings were used, including an average reporter S/N threshold of 10, and no scaling or normalization modes were applied. After peptides were identified and proteins were quantified, the results were then filtered to include those proteins for which a minimum of two unique peptides were identified. Log_2 protein ratios calculated in Proteome Discoverer were then fit to a normal distribution using non-linear (least squares) regression, and the mean and standard deviation values derived from the Gaussian fit of the ratios were used to calculate *p* values. Subsequently, *p* values were corrected for multiple comparisons by the Benjamini-Hochberg (B-H) method (25). Statistically significant changes were determined using the B-H method with an alpha (α) level of 0.05 (<5% FDR) (25).

The proteomics data has been deposited to the ProteomeXchange Consortium via the PRIDE partner repository (26) (accession number ProteomeXchange Consortium: PXD026831).

Ingenuity Pathway Analysis software (IPA, QIAGEN) was used to determine canonical signaling pathways and functional implications of the differential proteome expression. The statistical significance for each assignment was expressed by a corresponding *p*-values calculated using Fisher's exact test.

Western Blot. Macrophages were washed with PBS and lysed using ice cold CellLytic M Reagent (Sigma-Aldrich) supplemented with the Protease Inhibitor Cocktail (Set III, Calbiochem) and the Phosphatase Inhibitor Cocktail (Set I, Calbiochem). Protein concentrations were determined using the BCA Protein Assay (Pierce). Proteins were separated by SDS-PAGE on a 4-20% gel and transferred to nitrocellulose membranes. Membranes were blocked with 5% w/v milk in TBS with 0.1% Tween-20 for 1 h, and then incubated with primary antibody

overnight at 4°C in either 5% w/v milk in TBS with 0.1% Tween-20 or 5% w/v BSA in TBS with 0.1% Tween-20 (based on the manufacturer's recommendations) followed by incubation with secondary antibody in 5% w/v milk in TBS with 0.1% Tween-20 for 1 h. Protein bands were visualized using SuperSignal West Pico PLUS Chemiluminescent Substrate (Pierce) and HyBlot CL Autoradiography Film (labForce). Densitometric analysis of Western blots was performed with Fiji (27). See Supplemental Methods, Table S3 for information regarding antibodies used in this study.

Measurement of NO. NO (NO_2^-) concentrations were assessed 24 h p.i. with *H. pylori* by the standard Griess reaction (Promega)(2).

Flow Cytometry for CD11b and F4/80. Macrophages were infected or not with *H. pylori* PMSS1 for 24 h and then washed 3 times with PBS. Cells were fixed and permeabilized with CytoFix/CytoPerm (BD Biosciences) for 20 mins at 4°C, washed, and then labeled with anti-CD11b-FITC (BD Biosciences), 1/200, and anti-F4/80-PE, 1/200, (Thermo Fisher), for 20 min at 4°C in Perm/Wash Buffer. Cells were then washed 3 times and subsequently analyzed using flow cytometry. See Supplemental Methods, Table S3 for information regarding antibodies used in this study.

Glutathione Detection. Macrophages were infected or not with *H. pylori* PMSS1 for 24 h and then washed 3 times with PBS. Cells were then seeded into a white opaque 96-well assay plate at $1x10^4$ cells per 50 µl. Glutathione levels were assessed using the GSH-Glo Glutathione Assay kit (Promega) per the manufacturer's directions for cells in suspension.

Measurement of mitochondrial superoxide. Macrophages were infected or not with *H. pylori* PMSS1 for 24 h and then washed 3 times with Hank's balanced salt solution (HBSS) with calcium and magnesium. The cells were then incubated with HBSS containing 5 µM MitoSOX™ Red (Thermo Fisher) for 15 min at 37°C, washed once, and subsequently analyzed utilizing flow cytometry.

Cellular Respiration Profiling. Oxygen consumption rate (OCR) and extracellular acidification rate (ECAR) were measured using the Seahorse XFe96 Analyzer (Agilent). Differentiated BMmacs were seeded at $1x10^5$ cells per well in Seahorse XFe96 Cell Culture Microplates (Agilent) and infected or not with *H. pylori* PMSS1 (MOI 100) for 24 h. Cells were washed and incubated in Mitochondrial Stress Test Assay medium (1 mM sodium pyruvate, 2 mM glutamine, and 10 mM glucose in XF DMEM Medium (Agilent)) or Glycolysis Stress Test Assay

medium (2 mM glutamine in XF DMEM Medium (Agilent)) for 45 min at 37°C in the absence of CO_2. Mitochondrial oxidative phosphorylation and glycolytic function were assessed per the Mitochondrial Stress Test and Glycolysis Stress Test assay manuals (all Agilent). Briefly, for the Mitochondrial Stress Test assay, OCR was measured under basal conditions and after the sequential addition of the following drugs: 15 μM oligomycin (Cayman Chemicals), 10 μM fluoro-carbonyl cyanide phenylhydrazone (FCCP, Cayman Chemicals), and 5 μM rotenone with 5 μM antimycin A (both Sigma-Aldrich). For the Glycolysis Stress Test assay, ECAR was measured under basal condition and after the sequential addition of the following drugs: 10 mM glucose (Agilent), 10 μM oligomycin (Cayman Chemicals), and 500 mM 2-deoxy-glucose (2-DG, Cayman Chemicals). The drugs were loaded into calibrated XFe96 sensor cartridges (Agilent) and measurements were normalized to cell count. See Table S1 for information regarding reagents used in this study.

Table S1: List of reagents/kits used for this study

Reagent/Kit	Company	Identifier
Recombinant Murine M-CSF	PeproTech	Cat# 315-02
Dynabeads Untouched Mouse CD4 Cell Kit	Thermo Fisher	Cat# 11415D
LPS from *E. coli* O127:B8	Sigma-Aldrich	Cat# L4516
Recombinant Murine IFNg	PeproTech	Cat# 315-05
Recombinant Murine IL-4	PeproTech	Cat# 214-14
Recombinant Murine IL-10	PeproTech	Cat# 210-10
Oligo dT	Thermo Fisher	Cat#18418020
PowerUp SYBR Green Master Mix	Thermo Fisher	Cat# A25741
CellLytic M	Sigma-Aldrich	Cat# C2978
Protease Inhibitor Cocktail Set III	Calbiochem	Cat# 539134
Phosphatase Inhibitor Cocktail Set I	Calbiochem	Cat# 539131
SuperSignal West Pico PLUS Chemiluminescent Substrate	Thermo Fisher	Cat# 34577
S-(5-Adenosyl)-L-methionine chloride dihydrochloride	Sigma-Aldrich	Cat# A7007
Sardomozide	MedchemExpress	Cat# HY-13746
Streptavidin Particles Plus - DM	BD Biosciences	Cat# 557812
CytoFix/CytoPerm	BD Biosciences	Cat# 554714
GSH-Glo Glutathione Assay	Promega	Cat# V6911
MitoSOX™ Red Mitochondrial Superoxide Indicator	Thermo Fisher	Cat# M36008
Seahorse XFe96 FluxPak mini	Agilent	Cat# 102601-100
Seahorse XF DMEM	Agilent	Cat# 1035575-100
Seahorse XF 100 mM pyruvate	Agilent	Cat# 103578-100
Seahorse XF 1.0 M glucose	Agilent	Cat# 103577-100
Seahorse XF 200 mM glutamine	Agilent	Cat# 103579-100
Oligmycin Complex	Cayman Chemical	Cat# 11341
FCCP	Cayman Chemical	Cat# 15218
Rotenone	Sigma-Aldrich	Cat# R8875
Antimycin A	Sigma-Aldrich	Cat# A8674
2-DG	Cayman Chemical	Cat# 14325
TMTsixplex	Thermo Fisher	Cat# 90061
RNeasy Mini Kit	QIAGEN	Cat# 74106
RNeasy Micro Kit	QIAGEN	Cat# 74004
Superscript IV Reverse Transcriptase	Thermo Fisher	Cat# 18090010
BCA Protein Assay Kit	Pierce	Cat# 23225
Griess Reagent System	Promega	Cat# G2930
Fixation/Permeabilization Solution Kit	BD Biosciences	Cat# 554714
Pierce™ High pH Reversed-Phase Peptide Fractionation Kit	Thermo Fisher	Cat# 84868
CFSE	Thermo Fisher	Cat# 65-0850-84

Table S2: List of software/packages used for this paper

Software/Package	Company/Reference	Detail
Graphpad Prism	GraphPad Software (Versions 5.0 and 9.2)	https://www.graphpad.com/scientific-software/prism/
XCMS	Tautenhahn et al., 2012 (22)	https://xcmsonline.scripps.edu
Ingenuity Pathway Analysis (IPA)	QIAGEN	https://digitalinsights.qiagen.com/?promo=qiagen-ipa
Fiji (ImageJ)	Schindelin et al., 2012 (27)	https://imagej.net/Fiji
RStudio Desktop	RStudio	https://www.rstudio.com/products/rstudio/
fastp	Chen et al., 2018 (14)	
Salmon	Patro et al., 2017 (15)	
tximeta	Love et al., 2020 (16)	
DESeq2	Love et al., 2014 (17)	
clusterProfiler	Yu et al., 2012 (20)	
Dose	Yu et al., 2015 (21)	

Table S3: List of antibodies used for this study

Antibody	Company	Identifier
Rabbit polyclonal anti-NOS2	Millipore	Cat# ABN26; RRID: AB_10805939
Rabbit polyclonal anti-MyD88	Cell Signaling	Cat# 3699; RRID:AB_2282236
Rabbit polyclonal anti-NFkB p65	Millipore	Cat# PC138; RRID:AB_2179029
Rabbit monoclonal anti-pNFkB p65 S536	Abcam	Cat# ab76302; RRID:AB_1524028
Rabbit polyclonal anti-CD68	Boster Biological	Cat# PA1518
Rabbit monoclonal anti-CD3	Biocare	Cat# PME324AA
Rabbit monoclonal anti-Ly6G	Abcam	Cat# ab238132
Rabbit polyclonal anti-CTH	MyBioSource	Cat# MBS7047965
Rabbit monoclonal anti-IkBa	Thermo Fisher	Cat# MA5-15153; RRID:AB_10983739
Mouse monoclonal anti-pIkBa S32/36	Thermo Fisher	Cat# MA5-15224; RRID:AB_10981266
Mouse monoclonal anti-5-Methylcytidine	Bio-Rad	Cat# MCA2201; RRID:AB_324056
Mouse monoclonal anti-b-actin	Sigma-Aldrich	Cat# A5316 RRID:AB_476743
Goat anti-rabbit IgG, HRP-labeled	Jackson ImmunoResearch	Cat# 111-035-003; RRID: AB_2313567
Goat anti-mouse IgG, HRP-labeled	Jackson ImmunoResearch	Cat# 115-035-003; RRID: AB_10015289
Goat anti-rabbit IgG, Alexa fluor 488-labeled	Thermo Fisher	Cat# A-11008; RRID: AB_143165
Goat anti-mouse IgG, Alexa fluor 488-labeled	Thermo Fisher	Cat# A-10680; RRID:AB_2534062)
Anti-mouse F4/80, biotin-labeled	Thermo Fisher	Cat# MF48015; RRID:AB_10372665
Donkey anti-mouse IgG, Alexa fluor 555-labeled	Thermo Fisher	Cat# A-31570; RRID: AB_2536180
Anti-mouse CD11b, FITC Conjugate	BD Biosciences	Cat# 557396; RRID:AB_396679
Anti-mouse F4/80, PE Conjugate	Thermo Fisher	Cat# MF48004; RRID:AB_10372666
Anti-mouse CD68, PE Conjugate	BioLegend	Cat# 137014; RRID:AB_10612937
Monoclonal anti-mouse CD3e	Thermo Fisher	Cat# 16-0031-82; RRID:AB_468847
Monoclonal anti-mouse CD28	Thermo Fisher	Cat# 16-0281-81; RRID:AB_468920

Table S4: List of RT-PCR primers used for this paper

Target	Sequence
Cth	F: GCCAGTCCTCGGGTTTTGAA
	R: GCAAAGGCCAAACTGTGCTT
Cbs	F: TCATCCTGCCTGACTCTGTG
	R: CAGCTCTTGAACACGCAGAC
Tnf	F: CTGTGAAGGGAATGGGTGTT
	R: GGTCACTGTCCCAGCATCTT
Nos2	F: CACCTTGGAGTTCACCCAGT
	R: ACCACTCGTACTTGGGATGC
Il1b	F: ACCTGCTGGTGTGTGACGTTCC
	R: GGGTCCGACAGCACGAGGCT
Il12a	F: AAATGAAGCTCTGCATCCTGC
	R: TCACCCTGTTGATGGTCACG
Il12b	F: GAAAGACCCTGACCATCACT
	R: CCTTCTCTGCAGACAGAGAC
Cxcl1	F: GCTGGGATTCACCTCAAGAA
	R: CTTGGGGACACCTTTTAGCA
Mip2	F: GCCAAGGGTTGACTTCA
	R: TGTCTGGGCGCAGTG
Arg1	F: AAGAAAAGGCCGATTCACCT
	R: CACCTCCTCTGCTGTCTTCC
Il10	F: CCAAGCCTTATCGGAAATGA
	R: TCACTCTTCACCTGCTCCAC
Ifng	F: GGCCATCAGCAACAACATAAGCGT
	R: TGGGTTGTTGACCTCAAACTTGGC
Il17	F: ATCCCTCAAAGCTCAGCGTGTC
	R: GGGTCTTCATTGCGGTGGAGAG
Il6	F: AGTTGCCTTCTTGGGACTGA
	R: TCCACGATTTCCCAGAGAAC
Tgfb1	F: TCCTTGCCTGCGGAAGTG
	R: GGAGAGCATTGAGCAGTTCGA
Foxp3	F: GAGAGCAGGCAGTTCAGGAC
	R: CGGGAGCATATACCAGGCAC
Chil3	F: ACTTTGATGGCCTCAACCTG
	R: AATGATTCCTGCTCCTGTGG
Actb	F: CCAGAGCAAGAGAGGTATCC
	R: CTGTGGTGGTGAAGCTGTAG

SUPPLEMENTAL REFERENCES

1. Yang G, Wu L, Jiang B, Yang W, et al. H2S as a physiologic vasorelaxant: Hypertension in mice with deletion of cystathionine γ-lyase. *Science*. 2008;322(5901):587-590.
2. Hardbower DM, Asim M, Luis PB, Singh K, et al. Ornithine decarboxylase regulates M1 macrophage activation and mucosal inflammation via histone modifications. *Proc Natl Acad of Sci USA*. 2017;114(5):E751-E760.
3. Wilson KT, Ramanujam KS, Mobley HLT, Musselman RF, James SP, Meltzer SJ. *Helicobacter pylori* stimulates inducible nitric oxide synthase expression and activity in a murine macrophage cell line. *Gastroenterology*. 1996;111(6):1524-1533.
4. Chaturvedi R, Asim M, Hoge S, Lewis ND, et al. Polyamines impair immunity to *Helicobacter pylori* by inhibiting L-arginine uptake required for nitric oxide production. *Gastroenterology*. 2010;139(5):1686-1698.
5. Sierra JC, Asim M, Verriere TG, Piazuelo MB, et al. Epidermal growth factor receptor inhibition downregulates *Helicobacter pylori*-induced epithelial inflammatory responses, DNA damage and gastric carcinogenesis. *Gut*. 2018;67(7):1247-1260.
6. Hardbower DM, Singh K, Asim M, Verriere TG, et al. EGFR regulates macrophage activation and function in bacterial infection. *J Clin Invest*. 2016;9(126):3296-3312.
7. Gobert AP, Finley JL, Latour YL, Asim M, et al. Hypusination orchestrates the antimicrobial response of macrophages. *Cell Rep*. 2020;33(11):108510.
8. Stoyanov E, Mizrahi L, Olam D, Schnitzer-Perlman T, Galun E, Goldenberg DS. Tumor-suppressive effect of S-adenosylmethionine supplementation in a murine model of inflammation-mediated hepatocarcinogenesis is dependent on treatment longevity. *Oncotarget*. 2017;8(62):104772-104784.
9. Zabala-Letona A, Arruabarrena-Aristorena A, Martín-Martín N, Fernandez-Ruiz S, et al. MTORC1-dependent AMD1 regulation sustains polyamine metabolism in prostate cancer. *Nature*. 2017;547(7661):109-113.
10. Gobert AP, Latour YL, Asim M, Finley JL, et al. Bacterial pathogens hijack the innate immune response by activation of the reverse transsulfuration pathway. Torres, ed. *mBio*. 2019;10(5):e02174-19.
11. Dixon MF, Genta RM, Yardley JH, Correa P. Classification and grading of gastritis. The updated Sydney System. International Workshop on the Histopathology of Gastritis, Houston 1994. *Am Jl Surg Pathol*. 1996;20(10):1161-1181.
12. Lewis ND, Asim M, Barry DP, de Sablet T, et al. Immune evasion by *Helicobacter pylori* is mediated by induction of macrophage arginase II. *J Immunol*. 2011;186(6):3632-3641.
13. Asim M, Chaturvedi R, Hoge S, Lewis ND, et al. *Helicobacter pylori* induces ERK-dependent formation of a phospho-c-Fos c-Jun activator protein-1 complex that causes apoptosis in macrophages. *J Biol Chem*. 2010;285(26):20343-20357.
14. Chen S, Zhou Y, Chen Y, Gu J. fastp: an ultra-fast all-in-one FASTQ preprocessor. *Bioinformatics*. 2018;34(17):i884-i890.
15. Patro R, Duggal G, Love MI, Irizarry RA, Kingsford C. Salmon provides fast and bias-aware quantification of transcript expression. *Nat Methods*. 2017;14(4):417-419.
16. Love MI, Soneson C, Hickey PF, Johnson LK, et al. Tximeta: Reference sequence checksums for provenance identification in RNA-seq. *PLOS Comput Biol*. 2020;16(2):e1007664.
17. Love MI, Huber W, Anders S. Moderated estimation of fold change and dispersion for RNA-seq data with DESeq2. *Genome Biol*. 2014;15(12):550.
18. Huang DW, Sherman BT, Lempicki RA. Bioinformatics enrichment tools: Paths toward the comprehensive functional analysis of large gene lists. *Nucleic acids Res*. 2009;37(1):1-13.
19. Huang DW, Sherman BT, Lempicki RA. Systematic and integrative analysis of large gene lists using DAVID bioinformatics resources. *Nat Protoc*. 2009;4(1):44-57.

20. Yu G, Wang L-G, Han Y, He Q-Y. clusterProfiler: an R package for comparing biological themes among gene clusters. *Omi: A J Integr Biol*. 2012;16(5):284-287.
21. Yu G, Wang L-G, Yan G-R, He Q-Y. DOSE: an R/Bioconductor package for disease ontology semantic and enrichment analysis. *Bioinformatics*. 2015;31(4):608-609.
22. Tautenhahn R, Patti GJ, Rinehart D, Siuzdak G. XCMS Online: a web-based platform to process untargeted metabolomic data. *Anal Chem*. 2012;84(11):5035-5039.
23. Haug K, Cochrane K, Nainala VC, Williams M, et al. MetaboLights: a resource evolving in response to the needs of its scientific community. *Nucleic Acids Res*. 2020;48(D1):D440-D444.
24. Çelik-Uzuner S, Li Y, Peters L, O'Neill C. Measurement of global DNA methylation levels by flow cytometry in mouse fibroblasts. *In vitro Cell Dev Biol Anim*. 2017;53(1):1-6.
25. Thissen D, Steinberg L, Kuang D. Quick and easy implementation of the Benjamini-Hochberg procedure for controlling the false positive rate in multiple comparisons. *Journal Educ Behav Stat*. 2002;27(1):77-83.
26. Perez-Riverol Y, Csordas A, Bai J, Bernal-Llinares M, et al. The PRIDE database and related tools and resources in 2019: improving support for quantification data. *Nucleic Acids Res*. 2019;47(D1):D442-D450.
27. Schindelin J, Arganda-Carreras I, Frise E, Kaynig V, et al. Fiji: an open-source platform for biological-image analysis. *Nat Methods*. 2012;9(7):676-682.